

Thermoplastic Starch-Polypropylene reinforced with clay

Ana S. Abreu, M. Oliveira, A. V. Machado*

Institute of Polymers and Composites (IPC) and Institute of Nanostructures, Nanomodelling and Nanofabrication (I3N), University of Minho, Campus de Azurém, 4800-058 Guimarães, Portugal

* e-mail: avm@dep.uminho.pt

Abstract

In this study, bio-based blends of thermoplastic starch (TPS) and polypropylene grafted with maleic anhydride (PP-g-MA) without and with organoclay, Cloisite 30B, were prepared in an internal mixer. A TPS-g-PP copolymer was successfully obtained in melt and its formation was confirmed by SEM. The establishment of this copolymer creates an interpenetrating network leading an intercalated/exfoliated clay nanocomposite. Several analytical, angle X-ray diffraction (XRD), scanning and transmission electron microscopy (SEM, STEM) and dynamic mechanical analysis (DMA) were used to characterize the prepared materials. The nanocomposites mechanical properties were improved, showing an increase of about 11% for the nanocomposite when compared with the neat blend. Biodegradation studies performed in compost revealed good percentage of weight loss for the copolymer with clay addition.

Keywords: Bio-based polymer, polymer nanocomposites, thermoplastic starch

1 INTRODUCTION

The complete replacement with eco-friendly polymers is just impossible to achieve, therefore the use of biopolymers became crucial. Nowadays there is a great motivation in developing bio-based products and innovative process technologies that can reduce the dependence on fossil fuel and move to more sustainable materials basis. Bio-based nanocomposites are expected to possess improved strength and stiffness with little sacrifice of toughness, reduced gas/water vapor permeability, lower coefficient of thermal expansion, and an increased heat deflection temperature.^{1,2} Clay reinforcement of more environmentally friendly polymeric materials from bio-based sources with improved physical and mechanical properties, at very low filler loadings, has become the focus of significant research attention^{3,4}. Thermoplastic starch (TPS) is one of the most promising biodegradable polymer, it is completely degradable in soil and water and when blended with a non-biodegradable polymer it promotes its biodegradability.^{5,6} Since TPS cannot meet all the requirements of a packaging material, it is necessary to blend it with another polymer or add fillers to improve its properties. Polypropylene (PP) could be a

suitable polymer to blend with TPS once it exhibits an attractive combination of low weight and density, low cost, a heat distortion temperature above 100°C⁷. Due to

In this work, TPS, PP-g-MA and TPS/PP-g-MA (1:1) with 5 wt.% of Cloisite C30B nanocomposites were prepared by melt compounding using an internal mixer. The morphology and clay dispersion of the nanocomposites were observed by scanning electron microscopy (SEM), scanning transmission electron microscopy (STEM) and X-ray diffraction (XRD). Dynamic mechanical analysis (DMA) was used to investigate the mechanical performance and biodegradability was assessed by composting.

2 MATERIALS AND METHODS

2.1. Materials

Thermoplastic Starch (TPS), Mater-Bi®, was supplied by Novamont. Mater-Bi® is commercially available as blends of corn starch/PCL 30/70 (wt. %). Polypropylene-grafted-maleic anhydride (PP-g-MA, Poly-bond 3200) with a melting temperature around 160 °C and a MA content of 1 wt. %, was supplied by Crompton. Cloisite® 30B a montmorillonite (MMT) modified with a quaternary ammonium salt

(MT2EtOH = methyl tallowyl bis-2-hydroxyethyl ammonium chloride) was used as received.

2.2. Preparation of bio-based polymer nanocomposites

Compounds with different ratios of TPS and PP-g-MA (1:1) containing clay nanoparticles were prepared in the melt, in a Haake batch mixer (Rheocord 90; volume 60 cm³), equipped with two rotors running in a counter-rotating way.

2.3. Characterization

2.3.1 X-ray diffraction measurements (XRD) were performed to investigate the intercalation and exfoliation of C30B. The Bragg's law ($n\lambda = 2d_{001} \sin \theta$) was used to determine the clay interlayer distance d_{001} , where d is the spacing between silica layers of the clay (also called interlayer spacing), λ the wavelength of X-ray on the silica layer, and n is a whole number which represents the order of diffraction, taken 1 in our calculations.

2.3.2 Scanning electron microscopy (SEM) and scanning transmission electron microscopy (STEM) were carried out to analyze the nanocomposites morphology.

2.3.3 Dynamic mechanical analyses (DMA) experiments were performed in a TRITON apparatus in tension mode under the following parameters: frequency = 1 Hz; temperature scan rate = 2 °C/min; temperature range = -70 to 100 °C; free length = 15 mm and value tension = 15 μ m. At least two specimens of each sample were tested. Prior to mechanical measurements, plates were prepared by compression molding in a press (30 t for 1 minute at 180 °C).

2.3.4 Biodegradability test in compost was performed on TPS, TPS/C30B, TPS/PP-g-MA (1:1) and TPS/PP-g-MA (1:1)/C30B samples at 40 °C. Using rectangular samples (25 x 25 x 0.125 mm), they were placed in a composting medium made of soil, activated sludges from waste water treatment, straw and animal manure. The composting medium was kept in a relative humidity of approximately 50 – 70 %. Around 15 samples of each material were horizontally buried at 6 – 8 cm depth to guarantee aerobic degradation conditions at a horizontal distance of 5 – 6 cm between samples according to Fukushima et. al. ⁸. Based on the sample weight before and after

composting, the average percentage of residual weight for each material was calculated.

3 RESULTS AND DISCUSSION

When TPS and PP-g-MA in different ratios are melt mixing with C30B in the mixer, two chemical reactions can occur, allowing the formation of TPS-g-PP copolymer promoting an interpenetrating network creation. Such effect results in clay layers separation optimizing intercalation and/or exfoliation. The C30B clay structure has two hydroxyl groups (-OH), which can react with the PP-g-MA (-CO-O-CO-) to give an ester (-COO-) and an acid (-COOH). The acid group can then react with the second hydroxyl of the C30B clay (or coming from another part of the clay structure) to form a secondary ester and a water molecule ⁹. However, the hydroxyl groups presented in starch molecules, which are mainly constituted of amylose and amylopectin, can also react with the carbonyl of the maleic anhydride of the PP-g-MA to form TPS-g-PP copolymer.

Figure 1 presents SEM images of PP-g-MA/C30B and TPS/C30B nanocomposites. PP-g-MA with 5 wt.% of C30B presents a homogeneous dispersion of the clay in the magnifications presented. TPS with 5 wt.% of C30B exhibits a rougher surface, which can be explained by two factors. One is the possibility of voids creation that changes the surface roughness; two, the presence of an inorganic phase which affects the surface morphology (Figure 1).

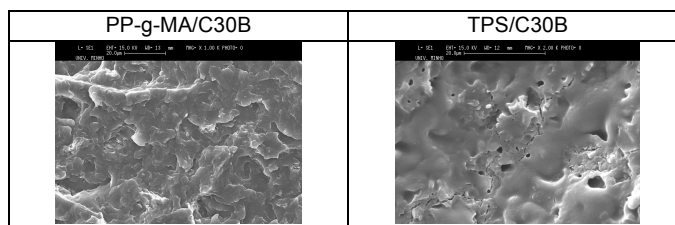


Figure 1. Morphology of PP-g-MA/C30B and TPS/C30B nanocomposites.

The effect of clay addition on the TPS/PP-g-MA (1:1) (Figure 2) blends, has a strong influence on their morphology. SEM micrographs of the nanocomposite exhibit a more homogeneous morphology when compared to TPS/PP-g-MA blend morphology (Figure 2). SEM results evidence that the polar character of organoclay C30B is a key factor for the higher interaction between TPS/PP-g-MA, which can also be enhanced if the reaction aforementioned occurs. C30B agglomerates cannot be observed, which point out to a good level of clay dispersion.

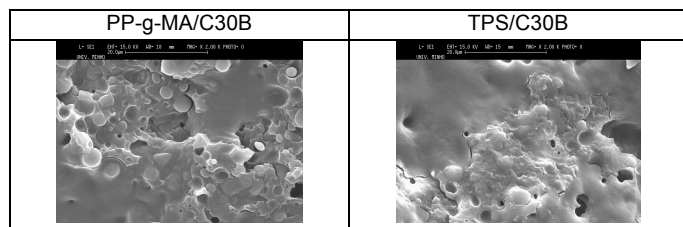


Figure 2. Morphology of TPS/PP-g-MA (1:1) blend and TPS/PP-g-MA (1:1) nanocomposites.

X-ray diffraction (XRD) analysis of neat C30B, PP-g-MA/C30B, TPS/PP-g-MA (1:1)/C30B, and TPS/C30B are presented in Figure 3. Based on XRD analysis, the space gallery was determined using Bragg law for the organoclay and the blends containing nanoclay. The mean interlayer spacing of the (001) plane (d_{001}) for the neat C30B clay solid obtained was 1.86 nm ($2\theta = 4.75^\circ$) (Figure 3). For all cases, it can be observed a significant shift of the reminiscent diffraction peaks to lower angles 2θ values relatively to C30B clay, indicating a intercalated and/or exfoliated (at least partially) dispersion of the clay platelets (Figure 3).

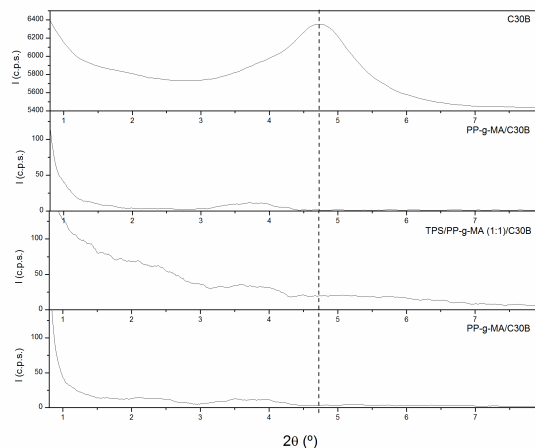


Figure 3. Morphology of TPS/PP-g-MA (1:1) blend and TPS/PP-g-MA (1:1) nanocomposites.

Applying the Bragg's law, the TPS/PP-g-MA (1:1) nanocomposite demonstrated to be the polymer matrix which has higher clay interlayer distance ($d_{001} = 2.47$ nm).

To assess the blends morphology without and with C30B, STEM analysis were performed for TPS/PP-g-MA (1:1) and for TPS/PP-g-MA (1:1)/C30B (Figure 4). In neat TPS/PP-g-MA (1:1) STEM image, two polymer phases are detected. With the addition of C30B, the dispersion of the clay promotes a better compatibility between the polymer matrices. The obtained results led us to conclude that the main phase TPS-g-PP has higher interfacial adhesion improving the dispersion/exfoliation of C30B.

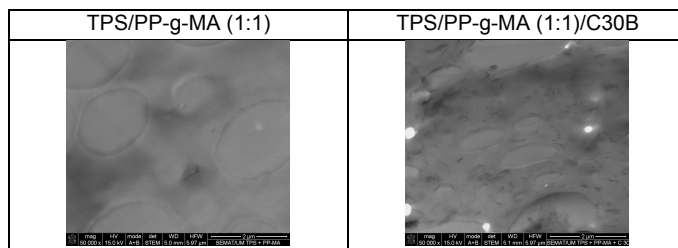


Figure 4. STEM micrographs of neat TPS/PP-g-MA (1:1) and TPS/PP-g-MA (1:1)/C30B.

The mechanical properties of TPS/PP-g-MA (1:1) are shown in Figure 5. An increase of storage modulus can be observed for the TPS/PP-g-MA (1:1) nanocomposite when compared to the neat corresponding matrix. The nanocomposite demonstrated an increase of dynamic storage modulus of about 11%. The effect of the clay addition to polymer matrices results in an increase of the modulus or stiffness via reinforcement mechanisms described by theories for composites¹⁰. A possible explanation for the improvement of the storage modulus even at temperatures above the room temperature could be the formation of a three-dimensional network of interconnected long silicate layers, strengthening the material through mechanical percolation¹¹.

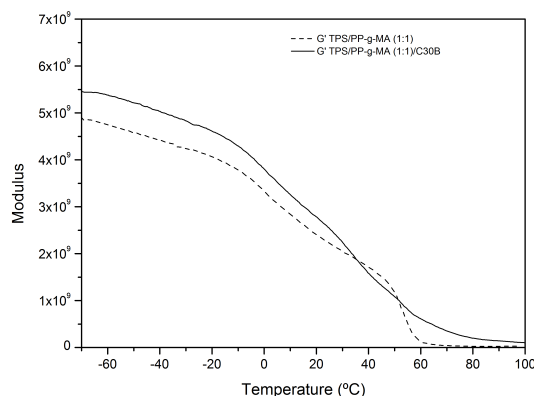


Figure 5. Modulus of TPS/PP-g-MA (1:1) and TPS/PP-g-MA (1:1) with 5% of C30B nanocomposite.

Biodegradation in compost for TPS, TPS/C30B, TPS/PP-g-MA (1:1) and TPS/PP-g-MA (1:1)/C30B samples were performed in 14 weeks at 40 °C (Figure 6). After 98 days of incubation in the composting system, the results revealed that TPS and TPS/C30B samples have the higher biodegradability when compared with TPS/PP-g-MA (1:1) and TPS/PP-g-MA (1:1)/C30B.

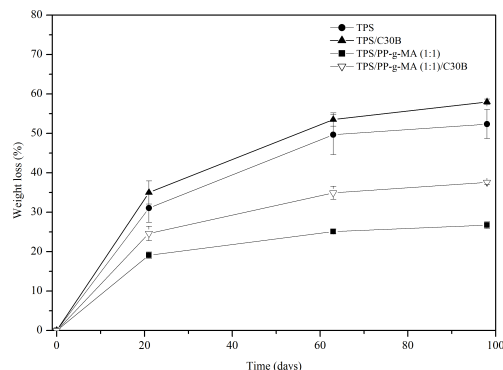


Figure 6. Composting results.

Biodegradation of TPS and TPS/C30B samples lost around 50 and 55 % of their weight, respectively. Through analysis of the biodegradation data of TPS/PP-g-MA (1:1) and TPS/PP-g-MA (1:1)/C30B, it can be concluded that the degradation rate and final biodegradation percentage was not so higher as for TPS and TPS/C30B. Biodegradation results of these samples showed 25% and 33% of weight loss at the end of composting for TPS/PP-g-MA (1:1) and TPS/PP-g-MA (1:1)/C30B. These results are explained by the presence of PP-g-MA, a non-biodegradable polymer. Nevertheless, such results are in agreement with the biodegradation results obtained for the TPS polymer, since the amount of TPS is present in half the amount in TPS/PP-g-MA (1:1). However, the effect catalytic of the clay on TPS and TPS/PP-g-MA was observed. Generally the presence of clay allows the acceleration of the biodegradation process.

4 CONCLUSIONS

Bio-based blends of thermoplastic starch (TPS) and polypropylene grafted with maleic anhydride (PP-g-MA) organoclay were successfully prepared. The effect of clay addition afforded intercalated/exfoliated bionanocomposites where mechanical properties were improved. Biodegradation results in compost revealed higher percentage of weight loss for the bio-based polymers containing clay.

5 ACKNOWLEDGMENT(S)

The authors acknowledge the n-STeP - Nanostructured systems for Tail, with reference NORTE-07-0124-FEDER-000039, supported by the Programa Operacional Regional do Norte (ON.2).

6 REFERENCES

- Alateyah, A. I.; Dhakal, H. N.; Zhang, Z. Y., Processing, Properties, and Applications of Polymer Nanocomposites Based on Layer Silicates: A Review. *Advances in Polymer Technology* **2013**, 32 (4).
- Tang, X.; Alavi, S., Recent advances in starch, polyvinyl alcohol based polymer blends, nanocomposites and their biodegradability. *Carbohydrate Polymers* **2011**, 85 (1), 7-16.
- Ojijo, V.; Sinha Ray, S., Processing strategies in bionanocomposites. *Progress in Polymer Science* **2013**, 38 (10-11), 1543-1589.
- Rhim, J.-W.; Park, H.-M.; Ha, C.-S., Bio-nanocomposites for food packaging applications. *Progress in Polymer Science* **2013**, 38 (10-11), 1629-1652.
- Mohammadi Nafchi, A.; Moradpour, M.; Saeidi, M.; Alias, A. K., Thermoplastic starches: Properties, challenges, and prospects. *Starch - Stärke* **2013**, 65 (1-2), 61-72.
- Hottle, T. A.; Bilec, M. M.; Landis, A. E., Sustainability assessments of bio-based polymers. *Polymer Degradation and Stability* **2013**, 98 (9), 1898-1907.
- Manias, E.; Touny, A.; Wu, L.; Strawhecker, K.; Lu, B.; Chung, T. C., Polypropylene/Montmorillonite Nanocomposites. Review of the Synthetic Routes and Materials Properties. *Chemistry of Materials* **2001**, 13 (10), 3516-3523.
- Fukushima, K.; Abbate, C.; Tabuani, D.; Gennari, M.; Camino, G., Biodegradation of poly(lactic acid) and its nanocomposites. *Polymer Degradation and Stability* **2009**, 94 (10), 1646-1655.
- Tessier, R.; Lafranche, E.; Krawczak, P., Development of novel melt-compounded starch-grafted polypropylene/polypropylene-grafted maleic anhydride/organoclay ternary hybrids. *Express Polymer Letters* **2012**, 6 (11), 937-952.
- Lee, K. Y.; Paul, D. R., A model for composites containing three-dimensional ellipsoidal inclusions. *Polymer* **2005**, 46 (21), 9064-9080.
- Lan, T.; Kaviratna, P. D.; Pinnavaia, T. J., On the Nature of Polyimide-Clay Hybrid Composites. *Chemistry of Materials* **1994**, 6 (5), 573-575.